PAN
ARCHIVES OF ACOUSTICS
Vol. **46**, No. 2, pp. 375–385 (2021)
DOI: 10.24425/aoa.2021.136590

Technical Note

Experimental Validation of the HVAC Humming-type Noise and Vibration in Model and Vehicle System Levels

Mohd Hafiz Abdul SATAR[(1)], Ahmad Zhafran Ahmad MAZLAN[(1)*], Muhd Hidayat HAMDAN[(1)], Mohd Syazwan Md ISA[(1)], Muhd Abdul Rahman PAIMAN[(2)], Mohd Zukhairi Abd GHAPAR[(2)]

[(1)] *The Vibration Lab, School of Mechanical Engineering*
Universiti Sains Malaysia
14300 Nibong Tebal, Penang, Malaysia
*Corresponding Author e-mail: zhafran@usm.my

[(2)] *Testing & Development, Vehicle Development & Engineering, Proton Holdings Berhad*
40000 Shah Alam, Selangor, Malaysia

(*received June 19, 2020; accepted January 18, 2021*)

The presence of noises in the vehicle cabin is an annoyance phenomenon which is significantly affected by the heating, ventilation, and air conditioning (HVAC) system. There are very limited studies reported on the specific type of noise characterisation and validation for both model and vehicle system levels. The present study developed a model of HVAC system that reflects the operation as in real vehicle, and the investigation of the HVAC components were carried out individually to determine which component contributes to the humming-type noise and vibration. The study was conducted under two conditions; idle speed of engine (850 rpm) and operating condition (850–1400 rpm). A ixed blower speed and full-face setting were applied throughout the experimental process. Three different sensors were used for the experiment, which are: accelerometer, tachometer, and microphone. From the results, the compressor and AC pipe components have contributed the most in generating the noise and vibration for both the model and vehicle systems. The findings also highlight that the humming-type noise and vibration were produced in the same operating frequency of 300–400 Hz and 100–300 Hz for idle and operating conditions, respectively, and this result was validated for both model and vehicle system levels.

Keywords: humming noise; HVAC system; vibration; compressor and AC pipe.

1. Introduction

The demands of consumers towards the automotive industry have evolved considerably over the last decade, as every finished marketable vehicle requires different levels of customer satisfaction to be met. The factors such as comfort and ergonomics have become essential criteria and potential research area, as no innovation concerning these factors can appear at the cost of the efficiency of vehicle operation. Comfort and operational efficiency are directly related to the heating, ventilation, and air conditioning (HVAC) system since the system operates while the vehicle is running (SINGH, MOHANTY, 2018). The energy accounted for this system is up to 30% of energy consumption from fuel and exceeds the level of consumption when driving in congested traffic and urban areas (SUBIANTORO *et al.*, 2014). In countries with hotter climatic conditions, like Brazil or India, more energy is consumed as it operates at high ventilation speeds to provide the desired comfort (LEITE *et al.*, 2009). Under these conditions, the tangible effects of the HVAC system become more significant.

Vibration and noise from the HVAC system are interrelated elements that have a substantial effect on the comfort of drivers and passengers. The vibration arising from the components of the system leads to noise generation, and the noises produced predominantly spread through the air in the vehicle interior space (QATU *et al.*, 2009; OKTAV, 2017). Several studies have proposed the existence of relationship between the vibration and noise, but the implemented

solutions are mostly on the fan. Wang *et al.* (2018) claimed that the noise generated can be related to the fan speed and suggested proportional relationship between the fan speed and noise generated. Further, Saeki *et al.* (1997) recommended changes to the specifications of fan and blade. The modifications in the design were able to reduce the turbulent airflow through the ducting and ventilation outlet with noise reduction up to 2 dBA.

Meanwhile, Toksoy *et al.* (1995) and Mavuri *et al.* (2008) described the effects of different operation settings on noise emission. The highest noise contribution was observed when the vents were set in full face and cold settings. The full cold setting allows maximum airflow from the blower, whereas for the full face, the blower is set towards the passenger face (Ene *et al.*, 2018). Mavuri *et al.* (2008) also mentioned that the noise is significantly affected by the seat material (i.e., fabric and leather). A continuous evaluation performed by Bennouna *et al.* (2018) determined that a passive absorber (i.e., foam) can reduce the noise in the interior space. The foams were placed at different locations of the HVAC components and aeraulic paths. Eilemann (1999) suggested that the foam thickness should be high. Limitations in the installation space only allowed thin layers of the foam (i.e., below 5 mm). Kurniawan and Rogers (2011) expanded the work to analyse the rubber seal to absorb the noise and further restrict the airflow induced whistle noise. As a result, rubber was used to stop airflow through a vertical orifice in between the HVAC housing wall and "V-shaped" seal tips.

Until date, several methods have been used to predict and validate the noise levels. Most of the reported methods have met various levels of success and most often use the computational fluid dynamics method. Détry *et al.* (2010) and Kim *et al.* (2016) simulated the generation and propagation of noise in the ducting system. The authors suspected the ducting system as a crucial component since it was related to the pressure separation and airflow obstacles. Pérot *et al.* (2013) used this method to evaluate the noises from various parts such as the face, feet, and rear vents. These components were critical and involved in the passage of the system to deliver and remove air. Another evaluation by Tiwari *et al.* (2009) on the flow behaviour and temperature considered several modes, such as defog and defrost, to observe the effects on airflow and temperature distribution throughout the system. Bel-Hassan *et al.* (2008) compared blower performances in stable and unstable flow conditions of operation. They claimed that stable flows were able to reduce pressure loss and provide uniform airflow. Hence, the better air splits at the duct outlets and proper mixing of hot and cold airs were observed. Aissaoui *et al.* (2015) validated the simulation model with experimental approach using real HVAC components. Both approaches were in good agreement, and the noise source was also identified in this study.

In a recent study by Mann *et al.* (2015), a discretisation method based on the continuum Boltzmann equation to simulate the noise propagation was developed, which is different from other studies using Navier-Stokes (Wang, 2010). The method has been applied in complex air conditional (AC) assemblies. In the experimental approach, it is common to use a microphone to record the sound from vibrating component and compare it with the noise of the models (Wiart *et al.*, 2010; Pallas *et al.*, 2011; Kierkegaard *et al.*, 2016). Additional verification methods are essential to characterise the source of the noise. In past studies, several methods such as particle image velocimetry (Lee *et al.*, 2011; Weyna, Mickiewicz, 2014), sound camera (Satar *et al.*, 2018; Martinez *et al.*, 2016), and sound diagnosis (Satar *et al.*, 2018) were used to correlate the data from the microphone. However, studies involved sound diagnosis are still limited in the literature.

Although remarkable progress has been made in the research and development of the HVAC systems, there are hardly studies that characterise noise types in the systems. Researchers have recognised that hissing noise in the HVAC system is one of the most prominent noises generated in it. It is produced when the liquid refrigerant is forced to flow through a small size orifice (Thawani *et al.*, 2013). Paiman *et al.* (2018) found that the evaporator component has contributed to this noise at the operating frequency of 4500–5000 Hz. Contrastingly, Thawani *et al.* (2005) found that the thermal expansion valve (TVX) was a major contributor to the hissing noise. The study was performed for a wider frequency range of 0 to 17.5 kHz and indicated the presence of hissing noise in the range of 6 kHz to 12.5 kHz. Another noise that originated from the HVAC system is a knocking noise. It is generated when the mounting bolts of any HVAC components system were loosened (Satar *et al.*, 2018). Based on the study by Sharma *et al.* (2012), knocking can lead to noise accompanied by a thermostat malfunction and this also related to the humming noise characteristics in the study that has been conducted on the vehicle system by Satar *et al.* (2018). They have successfully characterised the noise at different operating conditions such as different blower speeds and AC settings.

This study focused on the HVAC model development to characterise the humming-type noise and vibration. A lab-scale HVAC model has been created to imitate the real HVAC system operation in a vehicle. The root cause of the humming noise and vibration were determined by individual HVAC components investigation, and finally the results were validated with the vehicle HVAC system.

2. Methodology

2.1. Design and implementation of HVAC rig system

A model of completely assembled components of HVAC system was built on a rig structure as shown in Fig. 1. This model is aimed to produce similar real HVAC system conditions for the reliability of the test results. The rig structure was used as a fixed base to mount all the HVAC components. A commercial three-phase induction motor was used as a driver to the system by connecting the pulley to the compressor (Naidu *et al.*, 2005). The compressor is the main component in the system, which compresses and circulates low-pressure vapour that is drawn from the TVX. The liquid then flows through the condenser and fan, and the state is changed from a high-pressure vapour to liquid. Subsequently, the fluid flows through the dryer and TVX, where it is converted into low-pressure liquid. The fluid then flows towards an evaporator and blower, which changes the low-pressure liquid to low-pressure air. This low-pressure air is dispersed to the interior space of the vehicle and the processes are repeated continuously (Daly, 2006). In this study, a 12 V battery is used to provide the power supply to the HVAC system.

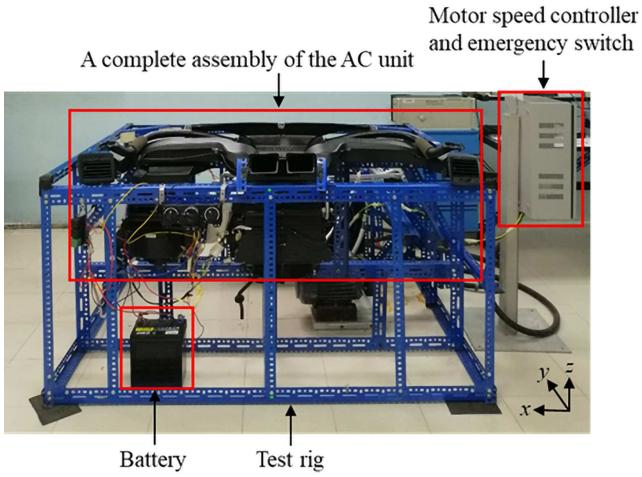

Fig. 1. Overall view of the HVAC model system and implementations.

2.2. Flow chart of noise and vibration measurement

This study comprises four main stages: problem identification and system analysis, measurement, data analysis of frequency content, and validation. The flow chart of the stages in the study is shown in Fig. 2.

2.2.1. Problem identification and system analysis

The noise occurrence was firstly identified based on the subjective feeling. In general, humming noise occurs at a low-frequency range with a moderate peak amplitude as a result of which it is heard as a high pitch sound (Song *et al.*, 2002). The problem identification was carried out for both the model and vehicle HVAC systems.

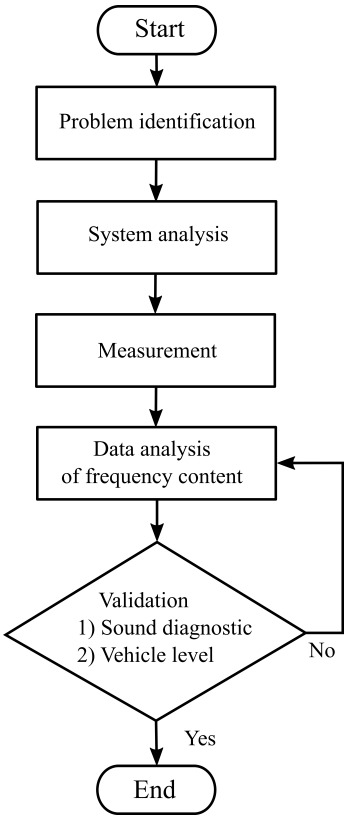

Fig. 2. Flowchart for investigation of the humming noise and vibration in HVAC system.

2.2.2. Measurement

Since the identified noise was based on the subjective feeling at the first stage, the noise and vibration measurements need to be done to verify the source. These measurements were carried out individually at each HVAC system component.

2.2.3. Data analysis

The recorded data were then analysed to identify the peak of the exploited response which might have produced the noise. In this stage, the frequency range obtained for each HVAC component was a preliminary postulation and needed to be verified in the consecutive stages.

2.2.4. Validation

The sound diagnosis tool was used to validate the presence of the noise and explain the reasons for the noise occurrence. All the results were then validated with the vehicle system and this serves as a reference for validating the newly developed HVAC model.

2.3. Experimental modal analysis (EMA)

EMA was carried out to determine the dynamic vibration characteristics of the HVAC components. It is an essential step in evaluating the effect of resonance, as the analysis can determine when the structure will oscillate and produce severe vibration (Ko *et al.*, 2011).

This analysis was initially carried out by defining the geometric model of the suspected HVAC components such as compressor, AC pipe, and the main structure (i.e., test rig), as shown in Fig. 3. As it can be seen in the figures, the AC pipe and compressor models were created with 3 and 8 nodes, respectively. As for the test rig, it was modelled with 18 nodes to create the actual shapes of the structure. An impact hammer which acts as the input force to excite the structure (Kistler type 9724A500) was used to hit the nodes accordingly. The output response was measured by an accelerometer (Kistler type 8776A50) that was placed at one of the nodes. All the tools were connected to the data acquisition (LMS SCADAS) system to compute the excitation and response signals. Then, the LMS Test Lab Software was used for the post-processing and displaying of the results.

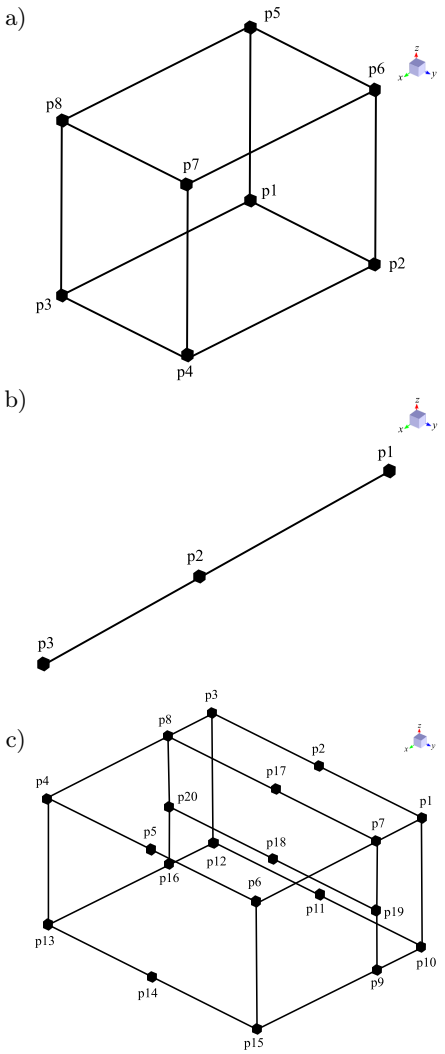

Fig. 3. Geometry models of: a) compressor, b) AC pipe, and c) rig structure.

2.4. Experimental setup for noise and vibration measurement

The noise and vibration measurements were conducted at both model and vehicle systems. Three sensors were used to measure the HVAC system components that generate the humming noise. As shown in Fig. 4, a tachometer (Monarch type SPSR-115/300) was mounted near the compressor to measure the engine speed at both idle and operating conditions. For the vehicle system, the engine speed was controlled by a foot pedal.

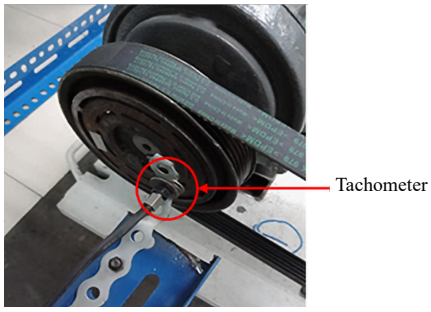

Fig. 4. Tachometer placed on the compressor of the HVAC model system.

A miniature-type accelerometer (Kistler type 877A50) was used to measure the vibration produced by the HVAC components. Figures 5 and 6 show the examples of the accelerometer mounted in the model and vehicle HVAC systems, respectively. The measurements were made for the components that were

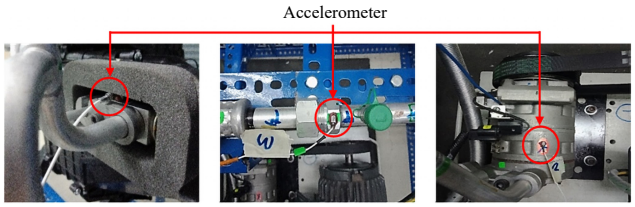

Fig. 5. Location of the sensors on (a) TVX, (b) AC pipe, and (c) compressor of the HVAC model system.

Fig. 6. Location of the sensors on (a) TVX, (b) AC pipe, and (c) compressor of the vehicle HVAC system.

suspected to cause the noise, as done in a previous study (Satar *et al.*, 2018). To verify the humming vibrational response among all the contributing HVAC components, the noise measurement was carried out using the microphone (BSWA type MA231). The microphone was placed 10 cm from each of the HVAC components, as suggested by Putner *et al.* (2013).

All the sensors were connected to the LMS SCADAS which is used to capture the respective dynamic signals from the sensors. The recorded data were then transferred to the LMS Test.Xpress for the analysis. The sound diagnosis tool available in the LMS Test.Xpress was utilised while filtering the order function to determine the humming noise characteristics. The data were examined within the frequency range of 0–500 Hz, the human audible range, as implied previously by Gren *et al.* (2012) and Sah *et al.* (2013).

2.5. Condition of noise and vibration measurement

Table 1 shows the working conditions for the vibration and noise measurements of the HVAC system. An idle condition was considered for vibration measurements in this study, which is a benchmark condition attributed from the findings by Mavuri *et al.* (2008). The condition was set to run and maintain an engine speed of 850 rpm, as part of the preliminary investigation to determine the root cause of the humming noise. Subsequently, a variation in the engine speed was applied for the operating condition. During the operating condition measurements, the engine speed was varied and it ran in the range of 850–1400 rpm. This operating speed was selected since the noise generated in the vehicle cabin was significant within this range, as suggested by Xie (2015). The blower speed of 1 (i.e., 2.5 m/s) was maintained for the measurement in both conditions.

Table 1. Working conditions and testing parameters.

Working conditions	AC status	Blower speed [m/s]	Locations
Idle	On	2.5	AC pipe, compressor, TVX, evaporator
Operating			

3. Results and discussion

3.1. EMA results

Figure 7 shows the frequency response function (FRF) graphs with their respective modes for three HVAC main components within the frequency range of 0–500 Hz, while Table 2 presents the first five modes corresponding to their natural frequency values. According to the figures, AC pipe, compressor, and rig structure have 3, 4, and 5 peaks of modes, respectively.

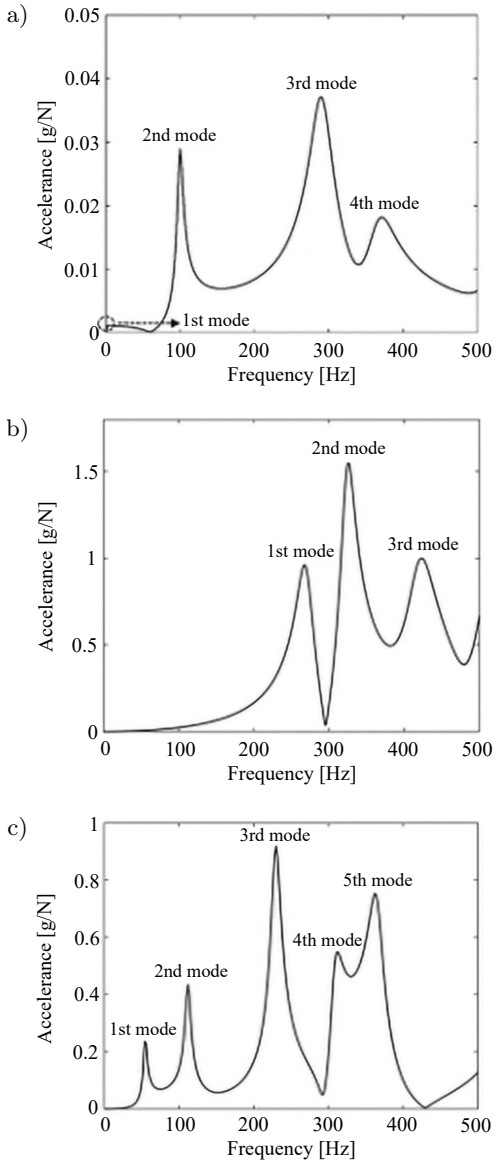

Fig. 7. FRFs of (a) compressor, (b) AC pipe, and (c) rig structure of the HVAC model system.

Table 2. Dynamic characteristics of the structures in the HVAC model system.

	Mode [Hz]				
	1	2	3	4	5
AC pipe	269.44	323.80	419.74	N/A	N/A
Compressor	10.31	99.76	290.81	365.14	N/A
Rig structure	56.66	112.23	229.60	307.56	365.02

For the compressor and rig structure, the third mode at 290.81 Hz and 229.60 Hz have higher accelerance output compared to the first two modes. On the contrary, the highest output for the AC pipe was observed at the second mode (i.e., 323.80 Hz). Based on these results, it is expected that the components will have severe vibration amplitude when operating close to the na-

tural frequencies, especially in the frequency range of 200–300 Hz. This is a typical problem with resonance of the structure, as found by Schillemeit and Cucuz (2002) and Prasanth *et al.* (2011).

3.2. Idle condition results

3.2.1. Vibration spectrum

Figure 8 presents the acceleration frequency response for the five major components of the HVAC model system in idle condition. It is observed that three components have contributed significant vibration within 300–400 Hz, namely, as motor, compressor, and AC pipe. The highest vibration was recorded from the motor approximately at 0.058 m/s^2, while for the compressor and AC pipe, the vibration amplitudes were approximately at 0.031 m/s^2 and 0.022 m/s^2, respectively. The highest vibration response was obtained in the range of 300–400 Hz. Meanwhile, moderate responses were found in the operating frequency above 450 Hz for all the components. The effect from the motor can be neglected since it is used to drive the compressor and not available in the real vehicle system.

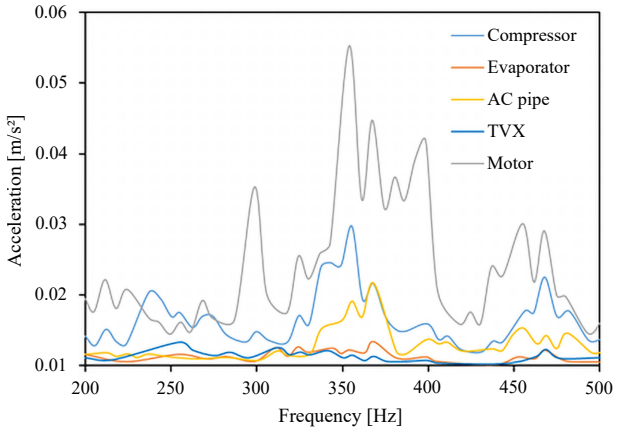

Fig. 8. Vibration frequency spectrum of main components for the HVAC model system (idle condition).

The vibration validation result with vehicle system is presented in Fig. 9. Since the vehicle system has more complicated structures, the spectrum was analysed in detail for all three directions (i.e., x, y, and z). From the figures it was found that the compressor has the highest vibration acceleration in the y axis direction with 0.81 m/s^2 of amplitude, while for the AC pipe, the highest peak occurred in the x axis direction with 0.89 m/s^2 of amplitude. Both peaks for compressor and AC pipe occurred within 300–400 Hz of the frequency range, similarly, as determined from the HVAC model system. These results can be related with the FRFs of compressor and AC pipe shown in Figs 7a and 7b, whereby both components were affected by

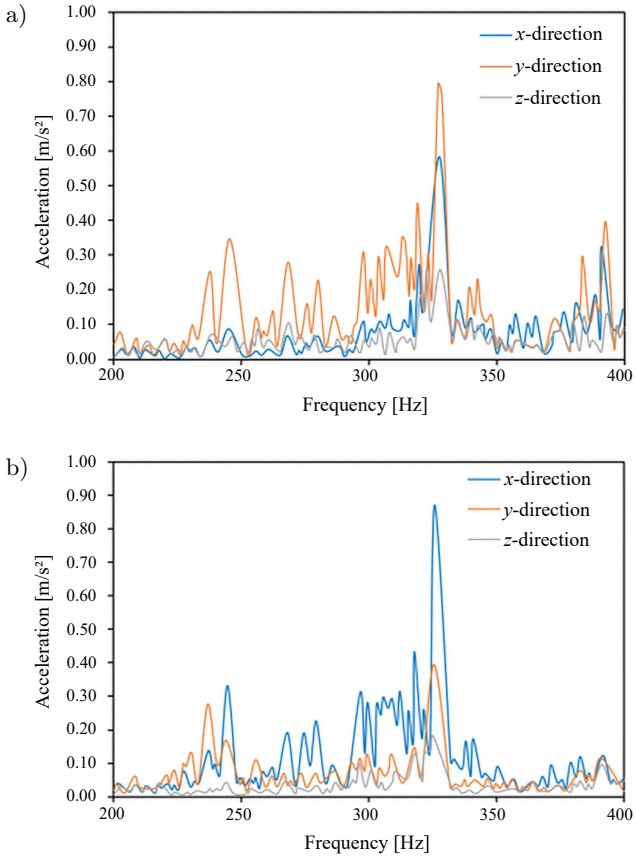

Fig. 9. Vibration frequency spectrum of (a) compressor and (b) AC pipe for the HVAC vehicle system (idle condition).

the natural frequencies of the structures and subsequently induced the humming-type vibration for the HVAC system.

3.2.2. 3D noise waterfall plot

Figures 10 and 11 show the 3D noise waterfall plot of the suspected HVAC components (compressor and AC pipe) for the model and vehicle systems, respectively. From Fig. 10, it was observed that the sound pressure level (SPL) increased significantly (up to 0.08 Pa(A)) from 0–150 Hz and subsequently reached zero gradients. As for the range of 300–400 Hz, the observation indicates that there are consecutive crests between 0–40 s of engine running time, as highlighted in the black-dash circle. The sound diagnosis tool was used to validate this postulation, and it was confirmed that the humming noise occurred within the frequency range of 300–400 Hz, as obtained previously by Satar *et al.*, 2019. This indicates that the humming noise can occur perpetually and be initiated after the compressor engagement. These results exhibited a comparable trend with the vehicle HVAC system, as shown in Fig. 11, whereby the significant crests were also found within the similar frequency range of 300–350 Hz.

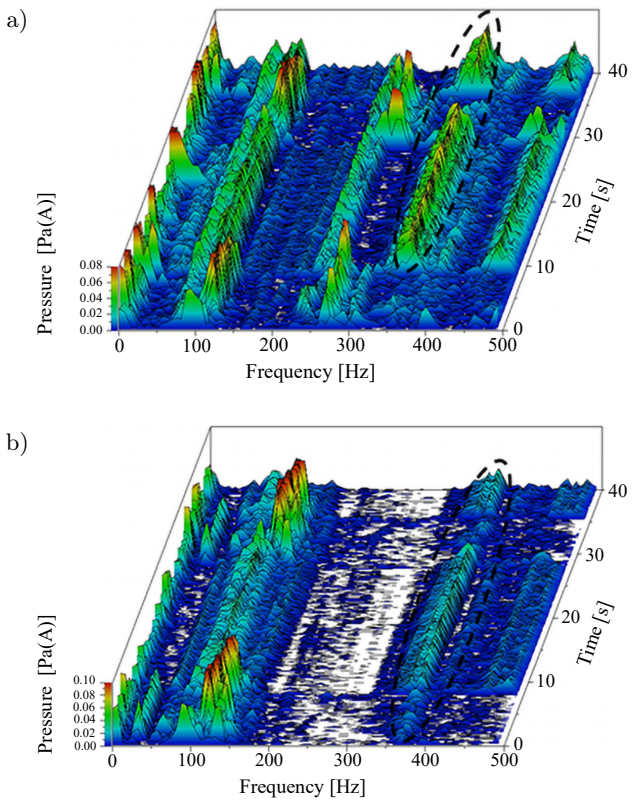

Fig. 10. Noise waterfall plot of (a) compressor and (b) AC pipe for the HVAC model system (idle condition).

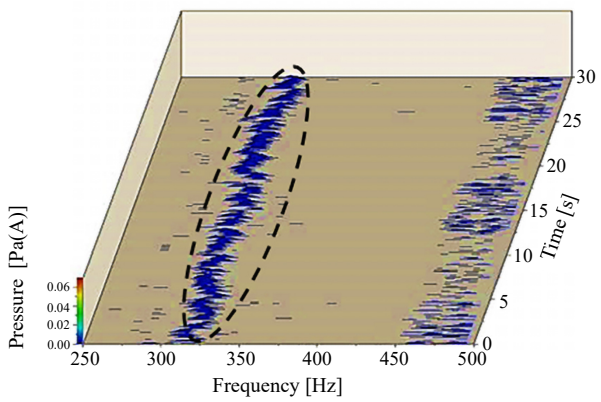

Fig. 11. Noise waterfall plot inside the cabin of HVAC vehicle system (idle condition).

Since both systems showed good agreement in terms of noise and vibration frequency spectrum results, further justification using the HVAC model system was carried out. The humming-type noise generation can be further explained based on the natural frequencies of the component structures. As shown in Fig. 7 previously, both compressor and AC pipe have the significant natural frequency peaks within 300–400 Hz, which further led to the occurrence of resonance phenomena. The studies done by Willemsen *et al.* (2009) and Brodie *et al.* (2012) did not mention the type of noise that could be attributed to this behaviour from the noise measurement in the vehicle cabin. From these results, it has been recognised that humming noises are present in the cabin.

3.3. Operating condition results

3.3.1. Vibration spectrum

Figure 12 shows the acceleration frequency response for the five major components of the HVAC model system in the operating condition. The result showed that all the components had considerable high vibration responses within the frequency range of 100–300 Hz. In comparison, the AC pipe witnessed the highest acceleration among all with 0.183 m/s^2 of amplitude, followed by the compressor with a relatively lower peak of acceleration. The TXV and evaporator exhibited the lowest amplitudes of vibration, like the trend observed for the idle condition, as shown in Fig. 8. Contrastingly, for the operating condition, the highest vibration response was observed in the frequency range of 100–300 Hz.

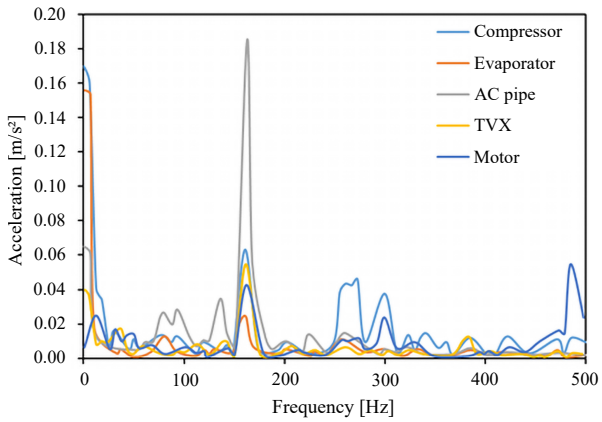

Fig. 12. Vibration frequency spectrum of the main components for the HVAC model system (operating condition).

The validation with the vehicle HVAC system is shown in Fig. 13. As one can see in the figures, the compressor and AC pipe exhibit the highest vibration in the y and x axis directions for the frequency range of 100–250 Hz, respectively. Above 250 Hz, the vibration amplitude started to deviate significantly and reached up to 0.95 m/s^2. This peak increment could be attributed to the natural frequency, which caused the resonance phenomena to the HVAC component structures, as observed in the earlier finding. This natural frequency effect also corresponded to the findings by Satar *et al.* (2019).

3.3.2. 3D order analysis

As engine is running, the components will be rotated and emit different vibration responses at certain amplitudes. Therefore, an order analysis was utilised to

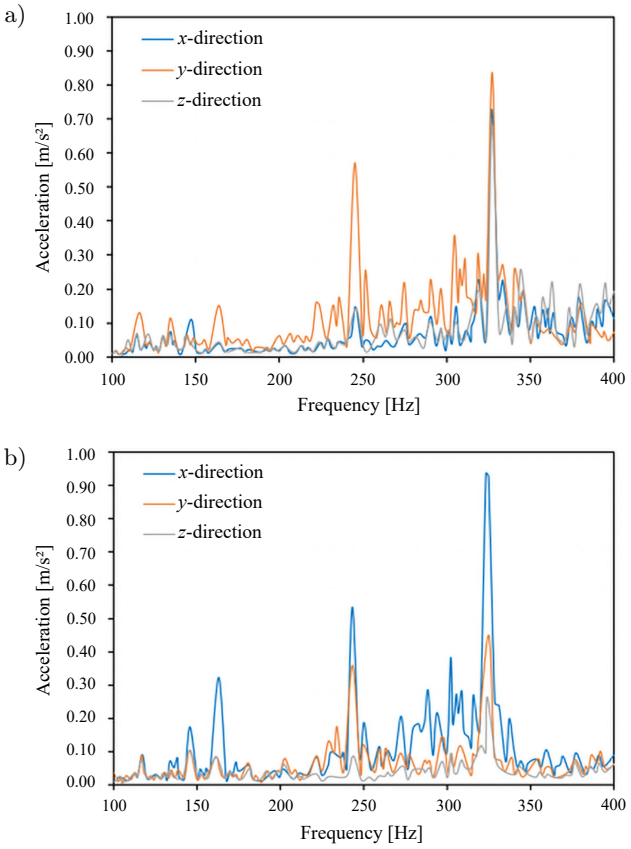

Fig. 13. Vibration frequency spectrum of (a) compressor and (b) AC pipe for the HVAC vehicle system (operating condition).

relate the engine speed (rpm) and vibration responses at different frequencies instead of using absolute frequency. The first order was set as a reference, and all orders were driven accordingly to the ratio of number of events per revolution based on the first event (Fyfe, Munck, 1997; Al-Badour *et al.*, 2011). In idle condition, there is no change in the engine speed, while for the operating condition, the increment of speed was conducted from 850 rpm to 1400 rpm.

The 3D order mapping of the humming noise contribution components is presented in Figs 14 and 15 for the HVAC model and vehicle systems, respectively. From Figs 14a and 14b, it was found that the compressor and AC pipe have the same order 11 (i.e., reddish spots) within the frequency range of 100–300 Hz. On comparing with vehicle system, the similar order 11 at the same operating frequency range was also obtained, as shown in Figs 15a and 15b. The major noise contribution components were determined as the compressor, followed by the AC pipe. After verifying with sound diagnosis tool, the humming-type noise was clearly defined within this frequency range of 100–300 Hz. The reddish spot in the vehicle system was more intense and noticeable compared to the idle system, which indicates that the noise is louder in the vehicle system.

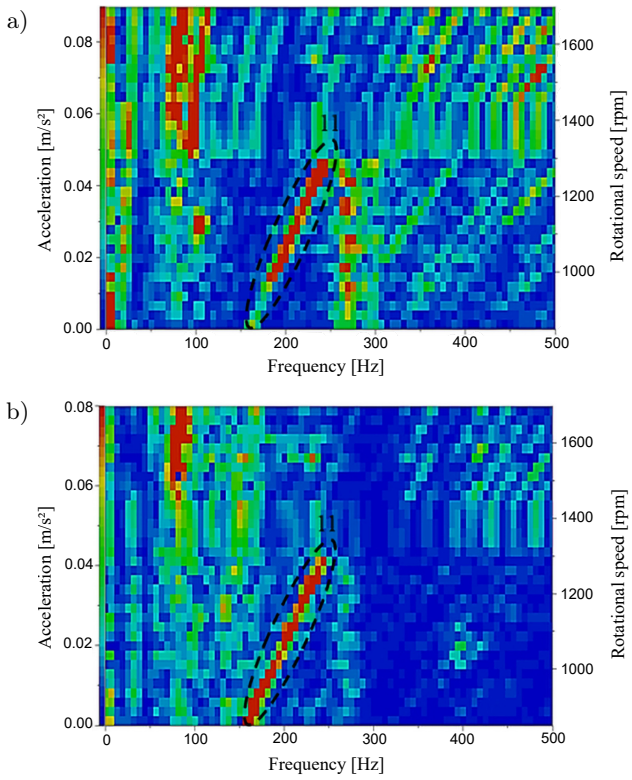

Fig. 14. Order mapping of (a) compressor and (b) AC pipe for the HVAC model system (operating condition).

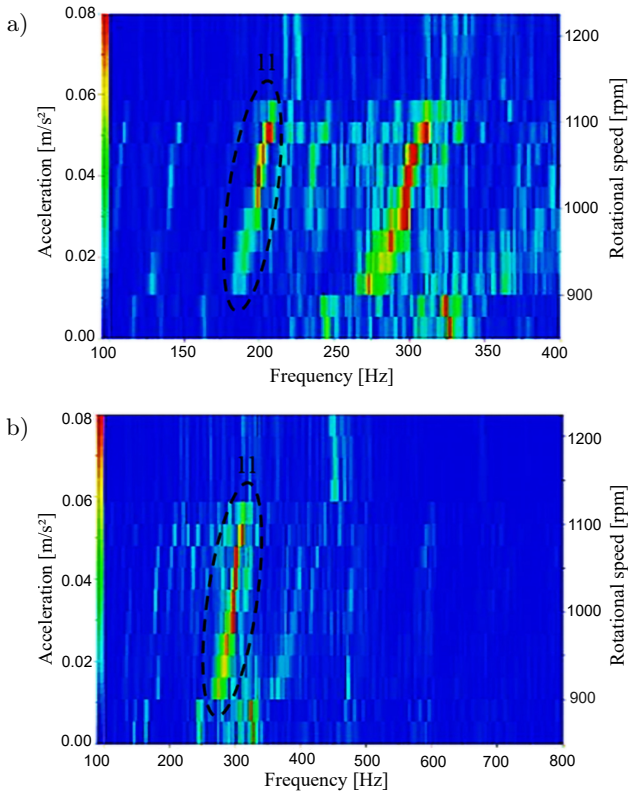

Fig. 15. Order mapping of (a) compressor and (b) AC pipe of the HVAC vehicle system (operating condition).

This humming noise phenomenon can be attributed to the vibration that has been transferred from the

compressor to the AC pipe, through the suction hose, as shown in Fig. 16, whereby all these components are linked together. This statement can be supported by the result of time domain vibration of the compressor during operation, as shown in Fig. 17. From the figure it is observed that there is a large vibration amplitude during the clutch engagement which contributes to the generating of humming noise. Thus, these results suggest that the humming noise constantly occurs only during the compressor clutch engagement period.

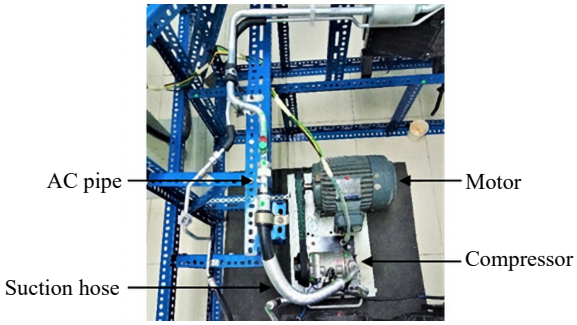

Fig. 16. Compressor and AC pipe directly linked by the suction hose.

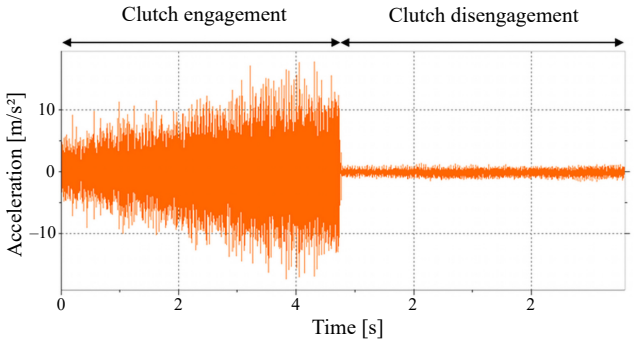

Fig. 17. Time domain vibration response of the compressor during operating condition.

3.4. Vibration and noise coherences

In this section, the humming-type noise and vibration data coherences are presented and verified for two major HVAC components (i.e., compressor and AC pipe) during the idle condition, as shown in Fig. 18. As it can be seen in the figure, the vibration amplitudes for the compressor and AC pipe are dominant within the frequency range of 300–400 Hz, as is highlighted in the yellow colour area of the figure. In the same frequency range, the noise that has been generated by both HVAC components is also shown by significant peaks. As verified using a sound diagnosis tool, the dominant peaks of vibration and noise within this range can be clearly indicated as the humming-type ones. The study done by Satar *et al.*, 2019 also agrees that this noise is significant within the 300–400 Hz of frequency, with the engine running in the idle condition.

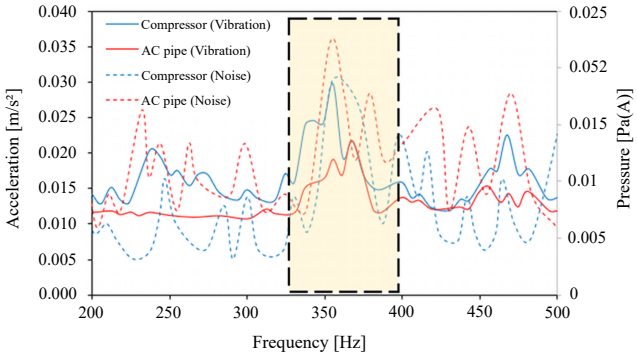

Fig. 18. Vibration and noise coherences of compressor and AC pipe during operating conditions.

4. Conclusion

In this study, the newly developed lab-scale HVAC model has demonstrated adequate evidence to be used as comparison with the real vehicle and investigating the root cause of the humming-type noise and vibration comprehensively. The humming noise and vibration were found existing in the frequency range of 300–400 Hz and 100–300 Hz for both idle and operating conditions, respectively. These frequency ranges coincided with the natural frequency values of two main HVAC components (i.e., compressor and AC pipe), which is believed to become the root cause of the humming noise problem. In comparison, both the model and vehicle systems managed to achieve good consensus, where the noise is mainly contributed by the compressor. From the order analysis results, the noise and vibration were clearly existing at order 11 for both model and vehicles systems during the increment of engine speed from 850-1400 rpm. It was also proved that the humming noise occurred during the engagement of compressor, it spreads towards the linked HVAC components such as AC pipe and becomes worse when the engine is running at a higher speed.

Acknowledgment

The authors would like to thank Universiti Sains Malaysia for offering financial assistance under RUI grant (1001/PMEKANIK/8014129). The work was also partly supported by Proton Holdings Berhad with laboratory facilities and technical support.

References

1. Aissaoui A. *et al.* (2015), Flow-induced noise optimization of SUV HVAC system using a lattice Boltzmann method, *SAE International Journal of Passenger Cars – Mechanical Systems*, **8**(3): 1053–1062, doi: 10.4271/2015-01-2323.
2. Al-Badour F., Sunar M., Cheded L. (2011), Vibration analysis of rotating machinery using time-frequency analysis and wavelet techniques, *Mechanical*

Systems and Signal Processing, **25**(6): 2083–2101, doi: 10.1016/j.ymssp.2011.01.017.

3. Bel-Hassan M., Sardar A., Ghias R. (2008), CFD simulations of an automotive HVAC blower: Operating under stable and unstable flow conditions, *SAE Technical Papers*, 2008-01-0735, doi: 10.4271/2008-01-0735.
4. Bennouna S., Matharan T., Cheriaux O. (2018), Automotive HVAC noise reduction, *SAE Technical Papers*, 2018-01-1519, doi: 10.4271/2018-01-1519.
5. Brodie B.R., Takano Y., Gocho M. (2012), Evaporator with integrated ejector for automotive cabin cooling, *SAE Technical Papers*, 2012-01-1048, doi: 10.4271/2012-01-1048.
6. Daly S. (2006), *Automotive Air Conditioning and Climate Control Systems*, Butterworth-Heimenn, Burlington, MA, doi: 10.1016/b978-0-7506-6955-9.x5000-9.
7. Détry S., Manera J., Detandt Y., D'Udekem D. (2010), Aero-acoustic predictions of industrial dashboard HVAC systems, *Noise Control Engineering Journal*, **59**(2): 177–185, doi: 10.3397/1.3545796.
8. Eilemann A. (1999), Practical noise and vibration optimization of HVAC systems, *SAE Technical Papers*, 1999-01-0867, doi: 10.4271/1999-01-0867.
9. Ene A., Catalina T., Vartires A. (2018), Determination of thermal and acoustic comfort inside a vehicle's cabin, [in:] *EENVIRO 2017 Workshop – Advances in Heat and Transfer in Built Environment, E3S Web of Conferences*, Vol. 32, 6 pages, doi: 10.1051/e3sconf/20183201002.
10. Fyfe K.R., Munck E.D.S. (1997), Analysis of computed order tracking, *Mechanical Systems and Signal Processing*, **11**(2): 187–205, doi: 10.1006/mssp.1996.0056.
11. Gren E., Farrall M., Mendonça F., Sandhu K. (2012), CFD prediction of aeroacoustic noise generation in a HVAC duct, [in:] *18th AIAA/CEAS Aeroacoustics Conference (33rd AIAA Aeroacoustics Conference)*, doi: 10.2514/6.2012-2068.
12. Kierkegaard A., West A., Caro S. (2016), HVAC noise simulations using direct and hybrid methods, [in:] *22nd AIAA/CEAS Aeroacoustics Conference*, doi: 10.2514/6.2016-2855.
13. Kim T.G., Hong S.Y., Song J.H., Kwon H.W. (2016), An empirical formulation for predicting HVAC system noise in offshore plants using computational analysis, *Noise Control Engineering Journal*, **64**(6): 716–726, doi: 10.3397/1/376414.
14. Ko Y. H., Mei L.X., Ripin Z.M. (2011), Tuned vibration absorber for suppression of hand-arm vibration in electric grass trimmer, *International Journal of Industrial Ergonomics*, **41**(5): 494–508, doi: 10.1016/j.ergon.2011.05.005.
15. Kurniawan D., Rogers E. (2011), Investigation of airflow induced whistle noise by HVAC control doors utilizing a 'V-shape' rubber seal, *SAE Technical Papers*, 2011-01-1615, doi: 10.4271/2011-01-1615.
16. Lee J.P., Kim H.L., Lee S.J. (2011), Large-scale PIV measurements of ventilation flow inside the passenger compartment of a real car, *Journal of Visualization*, **14**(4): 321–329, doi: 10.1007/s12650-011-0095-9.
17. Leite R.P., Paul S., Gerges S.N.Y. (2009), A sound quality-based investigation of the HVAC system noise of an automobile model, *Applied Acoustics*, **70**(4): 636–645, doi: 10.1016/j.apacoust.2008.06.010.
18. Mann A., Perot F., Meskine M., Kim M.S. (2015), Designing quieter HVAC systems coupling LBM and flow-induced noise source identification methods, [in:] 10th FKFS Conference *Progress in Vehicle Aerodynamics and Thermal Management*, Stuttgart.
19. Mavuri S.P., Watkins S., Wang X., St. Hill S., Weymouth D. (2008), An investigation of vehicle HVAC cabin noise, *SAE Technical Paper* 2008-01-0836, doi: 10.4271/2008-01-0836.
20. Martinez R.M., Snellen M., Simons D.G. (2016), Determination of aircraft noise variability using an acoustic camera, [in:] *23rd International Congress of Sound and Vibration: From Ancient to Modern Acoustics*, Athens, Greece.
21. Naidu M., Nehl T.W., Gopalakrishnan S., Würth L. (2005), Electric compressor drive with integrated electronics for 42 V automotive HVAC systems, *SAE Technical Papers*, 2005-01-1318, doi: 10.4271/ 2005-01-1318.
22. Oktav A. (2017), The effects of trunk cavity and air-gaps in the acoustic response of a passenger vehicle, *Archives of Acoustics*, **42**(3): 433–440, doi: 10.1515/aoa-2017-0045.
23. Paiman M.A.R. *et al.* (2018), Measurement of the hissing-type noise and vibration of the automotive HVAC system, [in:] *2018 International Conference on Vibration, Sound and System Dynamics (ICVSSD 2018), MATEC Web Conferences*, Vol. 217, Article No. 03002, doi: 10.1051/matecconf/201821703002.
24. Pallas M.A., Lelong J., Chatagnon R. (2011), Characterisation of tram noise emission and contribution of the noise sources, *Applied Acoustics*, **72**(7): 437–450, doi: 10.1016/j.apacoust.2011.01.008.
25. Pérot F. *et al.* (2013), HVAC noise predictions using a Lattice Boltzmann method, [in:] *19th AIAA/CEAS Aeroacoustics Conference*, doi: 10.2514/6.2013-2228.
26. Prasanth B., Wagh S., Hudson D. (2011), Alternator whining noise-a sound quality concern in passenger car, *SAE Technical Papers*, 2011-26-0018, doi: 10.4271/2011-26-0018.
27. Putner J., Lohrmann M., Fastl H. (2013), Analysis of the contributions from vehicle cabin surfaces to the interior noise, [in:] *42nd International Congress and Exposition on Noise Control Engineering, Inter-Noise 2013*, Innsbruck, Austria.
28. Qatu M.S., Abdelhamid M.K., Pang J., Sheng G. (2009), Overview of automotive noise and vibration, *International Journal of Vehicle Noise and Vibration*, **5**(1–2): 1–35, doi: 10.1504/IJVNV.2009.029187.

29. Saeki N., Kamiyama K., Uomoto M., Ishihara Y. (1997), Development of low noise blower fan, *SAE Technical Papers*, 971842, doi: 10.4271/971842.
30. Sah M., Srinivasan K., Mendonca F., Pai N. (2013), Prediction of HVAC system aero/acoustic noise generation and propagation using CFD, *SAE Technical Papers*, 2013-01-0856, doi: 10.4271/2013-01-0856.
31. Satar M.H.A. *et al.* (2018), Characterization of the humming type noise and vibration of the automotive HVAC system, *International Journal of Automotive and Mechanical Engineering*, **16**: 6634–6648, doi: 10.15282/ijame.16.2.2019.12.0499.
32. Satar M.H.A. *et al.* (2019), Application of the structural dynamic modification method to reduce the vibration of the vehicle HVAC system, *Journal of Physics: Conference Series*, **1262**: 012034, doi: 10.1088/1742-6596/1262/1/012034.
33. Schillemeit B., Cucuz S. (2002), Comparison of experimental NVH analysis techniques on automotive HVAC systems, *SAE Technical Papers*, 2002-01-1173, doi: 10.4271/2002-01-1173.
34. Sharma R.K., Parbhot C., Thakur S., Thakur V. (2012), Analysing reliability aspects of HVAC systems – A case, *Advanced Materials Research*, **488–489**: 1813–1817, doi: 10.4028/www.scientific.net/AMR.488-489.1813.
35. Singh S., Mohanty A.R. (2018), HVAC noise control using natural materials to improve vehicle interior sound quality, *Applied Acoustics*, **140**: 100–109, doi: 10.1016/j.apacoust.2018.05.013.
36. Song J., Bae S.Y., Yoon K. (2002), Query by humming: Matching humming query to polyphonic audio, [in:] *Proceedings. IEEE International Conference on Multimedia and Expo*, Lausanne, Switzerland, **1**: 329–332, doi: 10.1109/ICME.2002.1035785.
37. Subiantoro A., Ooi K.T., Stimming U. (2014), Energy saving measures for automotive air conditioning (AC) system in the tropics, [in:] *International Refrigeration and Air Conditioning Conference*, Paper 1361, http://docs.lib.purdue.edu/iracc/1361.
38. Thawani P., Liu Z., Venkatappa S. (2005), Objective metrics for automotive refrigerant system induced transients, *SAE Technical Papers*, 2005-01-2501, doi: 10.4271/2005-01-2501.
39. Thawani P.T., Sinadinos S., Black J. (2013), Automotive AC system induced refrigerant hiss and gurgle, *SAE International Journal of Passenger Cars – Mechanical Systems*, **6**(2): 1115–1119, doi: 10.4271/2013-01-1890.
40. Tiwari S., Agarwal R., Saxena P., Acre J. (2009), CFD-based design enhancements in passenger vehicle HVAC module, *SAE Technical Papers*, 2009-26-0058, doi: 10.4271/2009-26-0058.
41. Toksoy C. *et al.* (1995), Design of an automotive HVAC blower wheel for flow, noise and structural integrity, *SAE Technical Papers*, 950437, doi: 10.4271/950437.
42. Wang X. (2010), *Vehicle Noise and Vibration Refinement*, Woodhead Publishing Ltd, Melbourne.
43. Wang X., Watkins S., Charles S. (2018), Noise refinement solutions for vehicle HVAC systems, *SAE Technical Paper*, 2007-01-2184, doi: 10.4271/2007-01-2184.
44. Wiart C.C.D. *et al.* (2010), Validation of a hybrid CAA method: Noise generated by a flap in a simplified HVAC duct, [in:] *16th AIAA/CEAS Aeroacoustics Conference*, doi: 10.2514/6.2010-3995.
45. Weyna S., Mickiewicz W. (2014), Multi-modal acoustic flow decomposition examined in a hard walled cylindrical duct, *Archives of Acoustics*, **39**(2): 289–296, doi: 10.2478/aoa-2014-0033.
46. Willemsen A.M., Poradek F., Rao M.D. (2009), Reduction of noise in an excavator cabin using order tracking and ultrasonic leak detection, *Noise Control Engineering Journal*, **57**(5): 400–412, doi: 10.3397/1.3207865.
47. Xie X.-Z. (2015), Noise optimization design on the exhaust muffler of a special vehicle based on the improved genetic algorithm, *Journal of Vibroengineering*, **17**(8): 4625–4639.